

H33N-2193: Pore Scale Modelling of Carbon Capture and Sequestration

Ryan L Payton¹, Yizhuo Sun¹, Andrew Kingdon² and Saswata Hier-Majumder¹

Dept. Earth Sciences, Royal Holloway University of London¹, British Geological Survey²
ryan.payton.2015@live.rhul.ac.uk



- We present a reactive flow model describing mode of H₂CO₃ transport at both regional (2D) and micro (3D) scales.
 - Increasing porosity results in a shift from a channelised migration front to a tabular front.
 - Greater porosity and higher anorthite fraction both lead to higher CaCO₃ precipitation.
 - At the micro scale, throat radii <25μm control reduction in effective porosity by precipitation.

1. Introduction

Carbon capture and sequestration (CCS) is considered by many to be a major component in the solution for tackling anthropogenic climate change. The mode of transport of the reactive H₂CO₃ phase is of importance to understand how it affects mineralisation. We examine the impact of porosity and anorthite fraction on regional transport and anorthite fraction and connected porosity on micro scale transport.

2. Regional Scale CCS

$$\begin{aligned}
 (1) \quad \nabla \cdot \mathbf{u} &= 0 & (2) \quad \phi \mathbf{u} &= -\frac{k}{\mu} (\nabla p + \rho g \hat{\mathbf{z}}) \\
 (3) \quad (1 - \phi) \frac{\partial c_1}{\partial t} &= -\Gamma_1 & (4) \quad (1 - \phi) \frac{\partial c_2}{\partial t} &= \Gamma_2 \\
 (5) \quad \phi \frac{\partial c_0}{\partial t} + \phi \mathbf{u} \cdot \nabla c_0 &= \phi D \nabla^2 c_0 - \Gamma_0 + f_c \\
 (6) \quad \text{CaAl}_2\text{Si}_2\text{O}_8(s) + \text{H}_2\text{CO}_3(aq) &\rightleftharpoons \text{CaCO}_3(s) + \text{Al}_2\text{Si}_2\text{O}_5(\text{OH})_4(s)
 \end{aligned}$$

Equations 1-6: Regional scale numerical model governing equations.

$$\begin{aligned}
 (7) \quad \mathcal{D}a &= \frac{L \Gamma_0}{u_0} & (8) \quad \mathcal{P}e &= \frac{L u_0}{D}
 \end{aligned}$$

Equations 7&8: Definition of non-dimensional terms.

Fig. 1a

- Low porosity promotes formation of distinct channels.
- Greater porosity results in a planar migration front and a reduction in migration extent.

Fig. 1b

- Greater An fraction causes more reaction and consequently a reduced migration front.

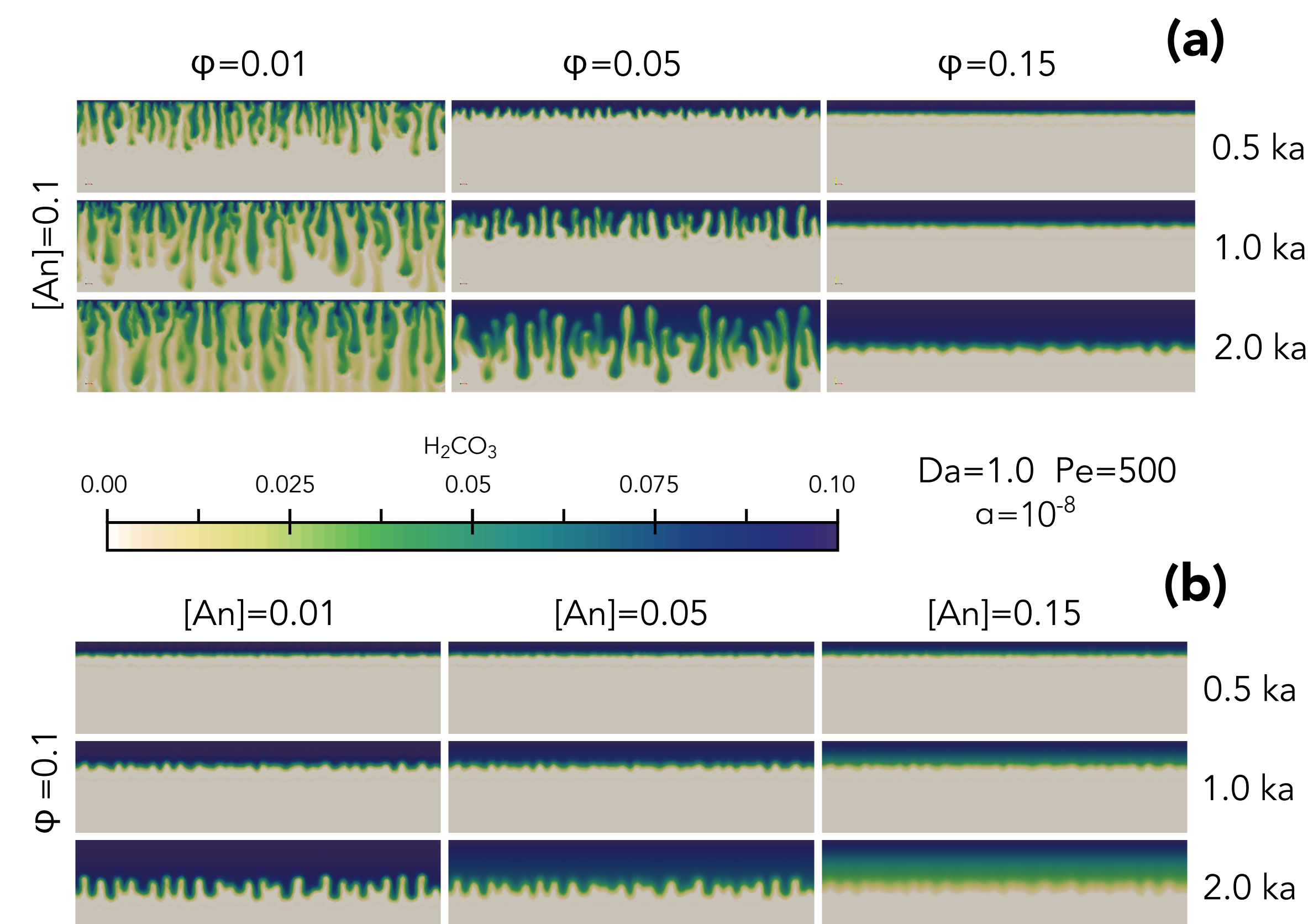


Figure 1: Top down migration front of H₂CO₃ under variable porosity (a) and An fraction (b) up to 2,000 years simulated time.

$$\begin{aligned}
 (9) \quad \nabla \cdot \mathbf{u} &= 0 & (10) \quad \mu \nabla^2 \mathbf{u} - \nabla p &= 0 \\
 (11) \quad \frac{\partial c_1}{\partial t} &= -\Gamma_1 & (12) \quad \frac{\partial c_2}{\partial t} &= \Gamma_2 \\
 (13) \quad \frac{\partial c_0}{\partial t} + \mathbf{u} \cdot \nabla c_0 &= D \nabla^2 c_0 - \Gamma_0
 \end{aligned}$$

Equations 9-13: Micro scale numerical model governing equations.

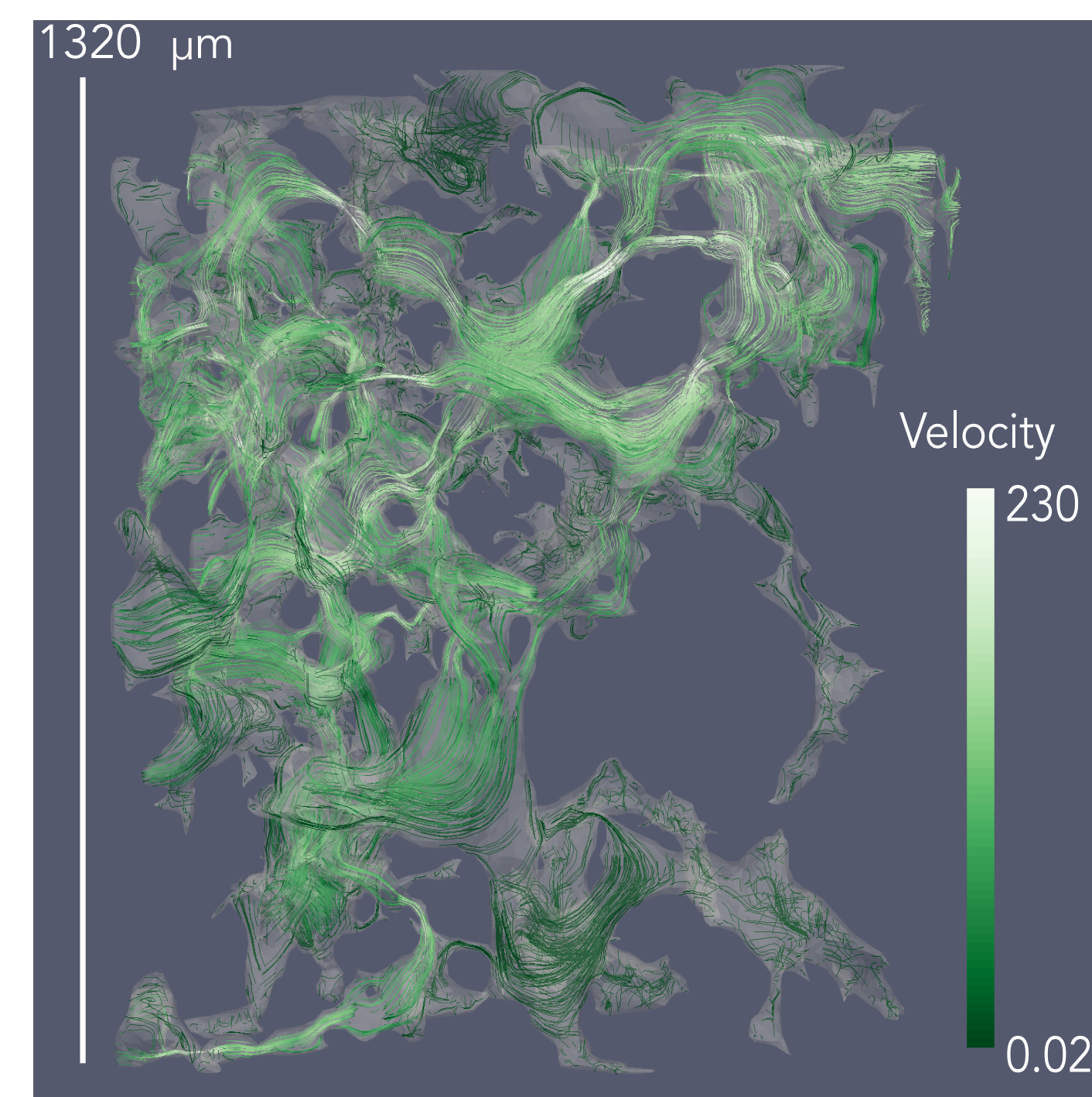


Figure 3: Nondimensional velocity streamlines through connected pore space. Colourmap is in logarithmic scale.

Fig. 2a

- Increasing An fraction results in a larger mass of CaCO₃ stored, increasing by ~300 MT from 5-25% An.
- Increasing reactivity (Da) results in a greater mass stored.

Fig. 2b

- Increasing porosity causes a greater mass of CaCO₃ to be stored.
- A shallower curve here suggests porosity is not as influential as An fraction on mass stored.

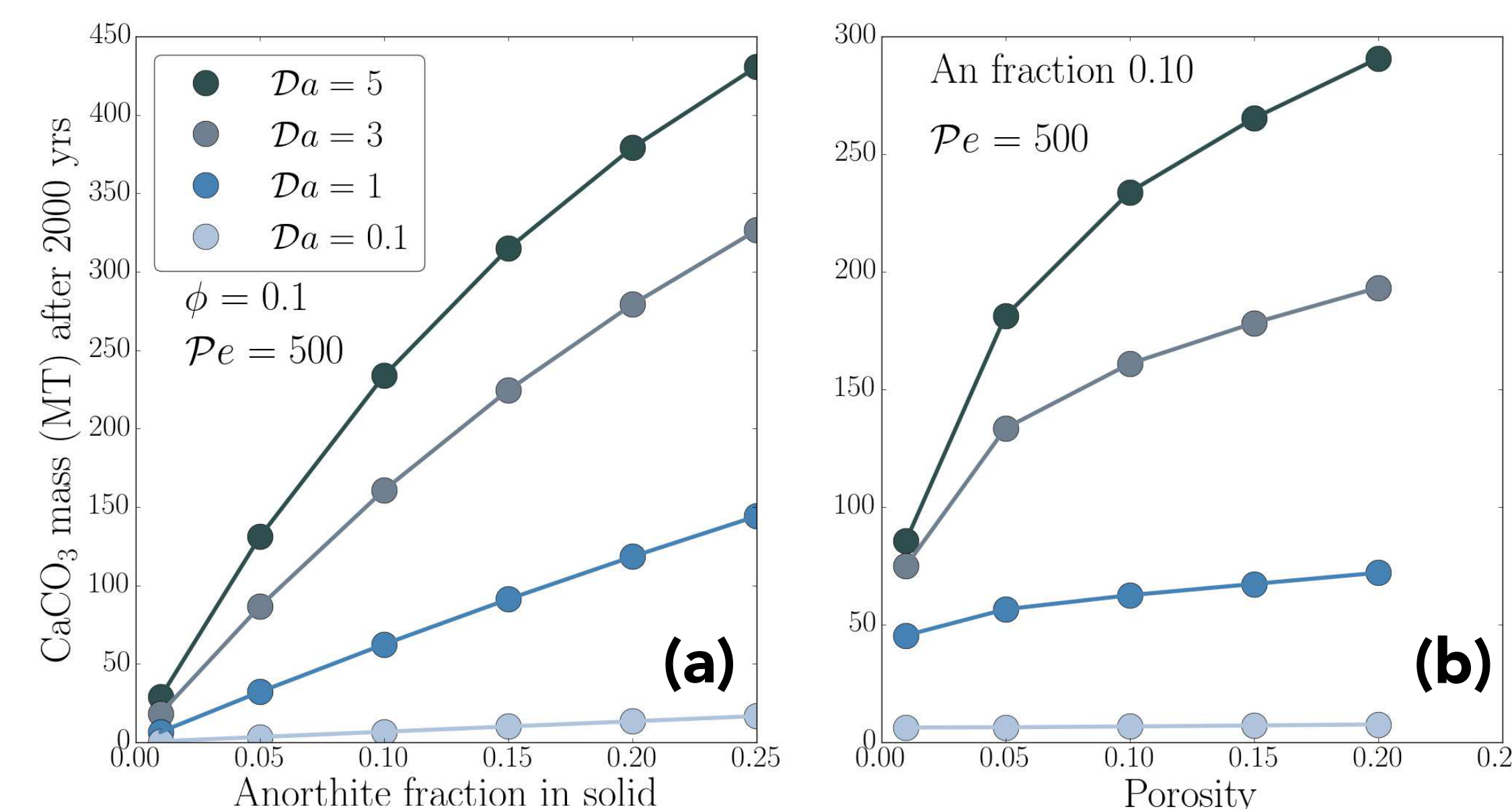


Figure 2: The relationship between An frac (a) and porosity (b) with mass of CaCO₃ precipitated from the H₂CO₃ and Ca reaction. Greater Da increases the strength of this reaction.

3. Micro Scale CCS

We imaged a sample of Brae sandstone from the North Sea using μCT. We investigate the mode of transport of H₂CO₃ under groundwater flow conditions through connected porosity.

Fig. 3

- Main flow channels are highlighted in brighter colours.
- Deprived areas are shown by darker colours.
- A clear central highway is seen despite complete connectivity.

Fig. 4

- Highlights the CaCO₃ concentration as a function of time.
- The main channels fill rapidly.
- Low velocity channels are deprived far longer.

Fig. 5

- A narrow throat causes a CaCO₃ build up behind it.
- It takes far longer for peak concentration to be reached beyond the bottleneck.
- This geometry is likely to become isolated and reduce effective porosity.

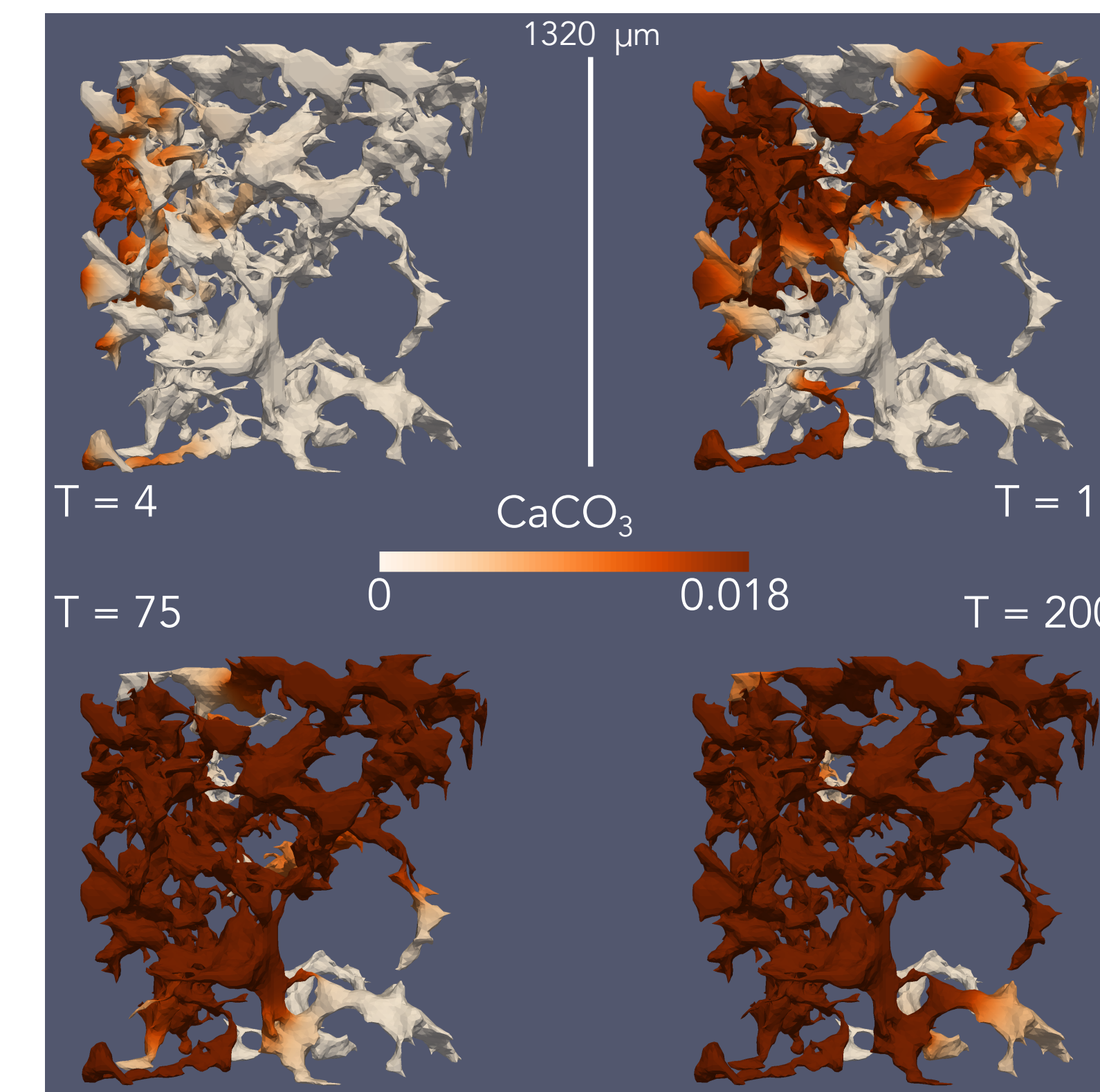


Figure 4: Whole sample CaCO₃ concentration map. Flow is L-R. Da = 0.1, An = 0.05.

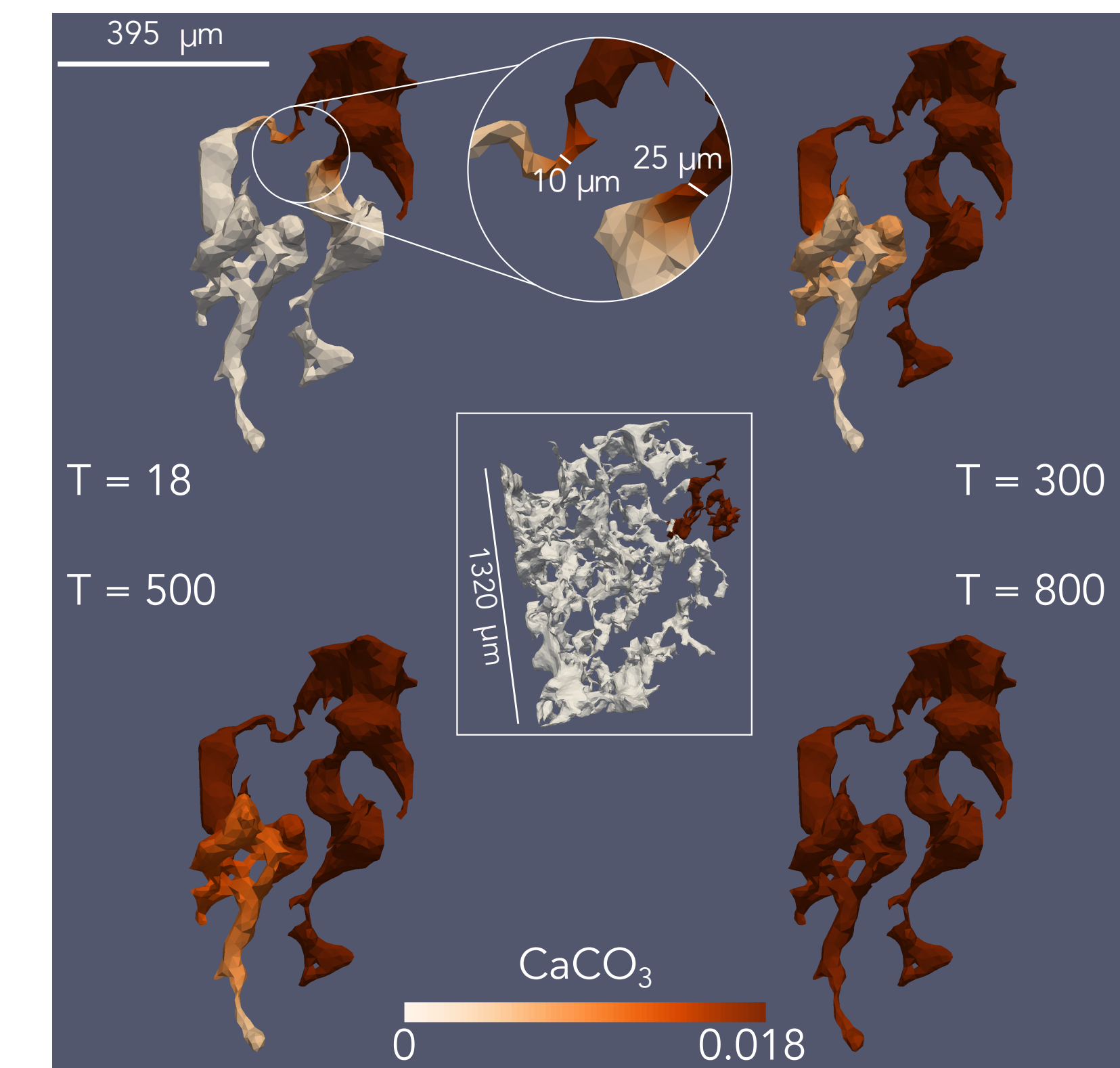


Figure 5: Subsample CaCO₃ concentration map. Flow is from the upper right corner. Da = 0.1, An = 0.05.

Fig. 6

- As the An fraction increases, the peak CaCO₃ concentration does too.
- The large difference in peak CaCO₃ between 5% and 15% shows the importance of lithology in choosing a target formation for CCS.

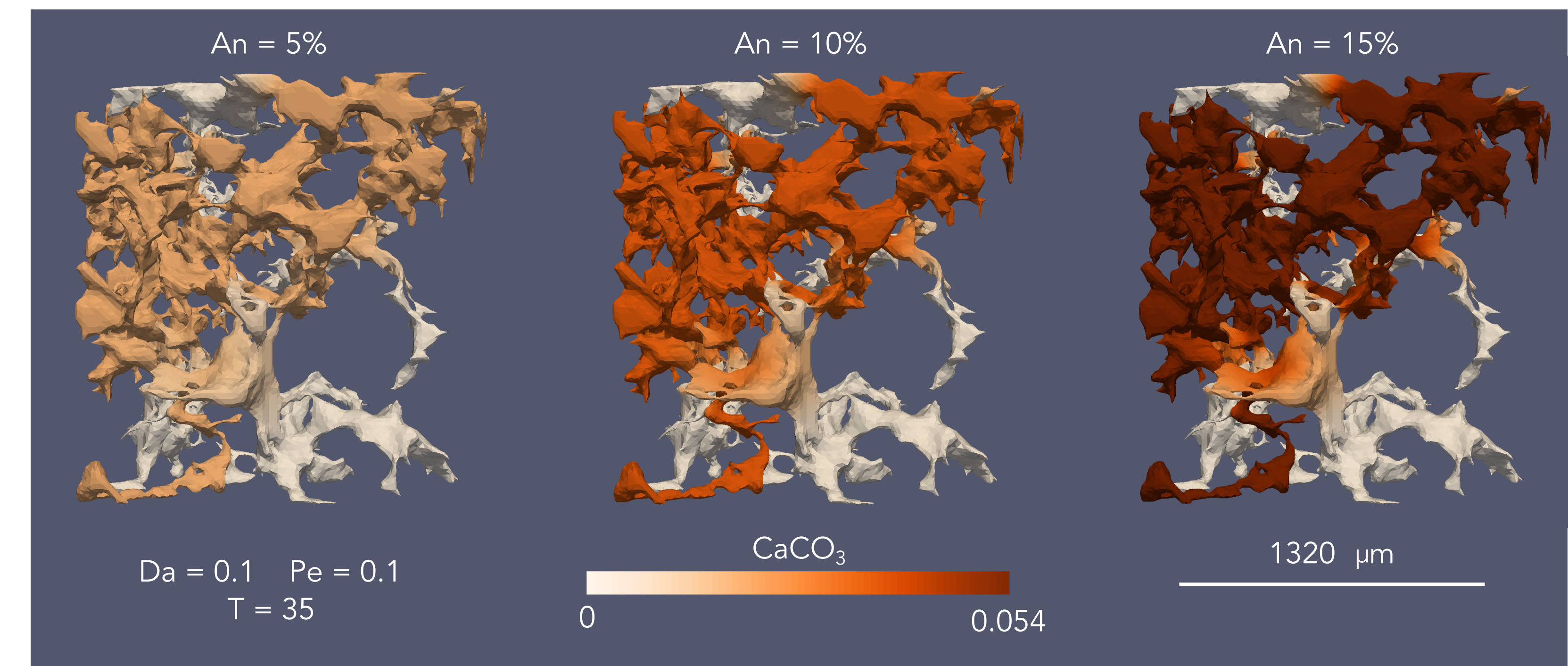


Figure 6: CaCO₃ concentration map for variable An fraction. Flow is from L-R. Da = 0.1.

4. Future Work

1. A method of upscaling of the micro scale model will be developed by simulating CaCO₃ precipitation in μCT images with different porosity.
2. Dimensional analysis of micro scale results to determine mass of CaCO₃ stored in the study volumes.
3. Validation of the micro model through simulation on cemented samples with the cement phase removed to compare precipitation choke points.

Acknowledgements

This work is financially supported by a NERC studentship with the London NERC DTP. We would also like to thank Oracle for a cloud computing grant. Further thanks to Frank Lehane at RHUL for technical computing support throughout the project.